Thermal and Physical Properties of PVA-PEO Films Reinforced with Manganese Chloride Tetrahydrate

Rana S. Mahmood[1], Sabah A. Salman[2] and Alaa H. Hassien[1]
[1]General Directorate of Education Diyala, 32001 Baqubah, Iraq
[2]Department of Physics, College of Science, University of Diyala, 32001 Baqubah, Iraq
{ranasaadmahmood82 , alaahameed336@gmail.com}, pro.dr_sabahanwer@yahoo.com

Keywords: Blend, Thermal Conductivity, Glass Transition Temperature, Crystalline Melting, True Density.

Abstract: This work describes the procedures for producing pure polymeric blend films (PVA-PEO) and polymeric blend films enhanced with $MnCl_2 \cdot 4H_2O$ salt at different weight ratios (10, 20, 30, 40, and 50 wt%) by the solution casting process. We examined the impact of the salt weight ratio on the thermal properties of all the reinforced polymeric mix films. The thermal conductivity coefficient (k) increases to 0.000474 W/m·°K when the weight ratio of added $MnCl_2 \cdot 4H_2O$ salt is 10 wt%. Subsequently, the thermal conductivity coefficient continues to decrease when the weight ratio of additional $MnCl_2 \cdot 4H_2O$ salt increases. The inconsistency in the coefficient value may be attributed to the heterogeneity of the matrix material, stemming from the significant surface area of the $MnCl_2 \cdot 4H_2O$ salt. The differential scanning calorimetry (DSC) analysis of all reinforced polymeric blend films revealed that the glass transition temperature (T_g) and crystalline melting temperature (T_m) values demonstrate an erratic decrease as the weight ratio of added salt increases, with the pure polymeric blend film [PVA-PEO] exhibiting a T_g of 167.94 °C. The impact of the salt weight ratio on real density, apparent porosity, and water absorbance in all reinforced polymeric mix films was investigated. The results demonstrated that actual density rose with a raised salt weight ratio, whereas apparent porosity and water absorbance diminished as the salt weight ratio escalated.

1 INTRODUCTION

Polymers have garnered considerable interest owing to their extensive array of applications. The combination of diverse polymers or inorganic substances with polymers represents a strategic method to enhance material performance, enabling the development of innovative composite systems that improve the effectiveness of the original mixture [1]. The blending of multiple polymers is a technique employed to create innovative materials with unique properties, primarily influenced by the attributes of the individual homopolymers and the composition of the mixture [2]. The advancement of conductive polymers has introduced a novel aspect to the current epoch. Polymers are categorized as thermally responsive, pliable, electrically insulating, and amorphous substances. Electrically conductive polymers are optimal for diverse applications, as numerous properties mitigate issues commonly associated with conventional materials, such as corrosion, weight, matrix incompatibility, and environmental stability. In addition to their corrosion resistance and lightweight properties, other critical attributes of conducting polymers can be tailored for various applications. The strength-to-weight ratio, potential, and corrosion resistance of conducting polymers confer advantages over metals. Polymers are commonly recognized for their insulating properties, which are attributed to the Covalent bonding in saturated carbon compounds. Researchers have investigated the possibility of converting insulating polymers into conducting or semiconducting materials through structural modifications and the incorporation of additives, aiming for attributes such as low density, ease of fabrication, design flexibility, and decreased energy requirements for processing and manufacturing [3]. Previous studies have demonstrated that the integration of PVA with other polymers or the addition of inorganic ions can markedly enhance the characteristics of the polymer matrix [4]. Additional analysis of PVA/PEO mixtures demonstrated that altering the PEO ratio markedly influenced the glass transition temperature (T_g) and crystalline melting temperature (T_m) of the films, emphasising the critical role of polymer composition in thermal properties [5]. This research endeavours to produce polymeric composite films composed of a blend of polyvinyl alcohol (PVA) and polythene oxide (PEO), reinforced with manganese chloride ($MnCl_2 \cdot 4H_2O$) at different weight ratios (10, 20, 30, 40, 50 wt%) via the casting technique. Investigate the impact of varying weight ratios of manganese chloride ($MnCl_2 \cdot 4H_2O$) on diverse structural parameters, encompassing the thermal conductivity coefficient (k), glass transition temperature (T_g), crystalline melting temperature (T_m), actual density, apparent porosity, and water absorption.

2 MATERIALS AND METHODS

PVA is a polymer characterised as an odourless, non-toxic white granule that dissolves rapidly in purified water. The molecular weight spectrum spans from 13,000 to 23,000 g/mol. Polythene oxide [PEO], with molecular weights ranging from 150,000 to 10 million, is produced through the polymerisation of ethylene oxide. PEO holds significance across diverse industrial environments. Figure 1 illustrates the structural formula of the polymer [6], [7]. Anhydrous manganese chloride is a chemical compound with the molecular formula $MnCl_2$, distinguished from its hydrated form, $MnCl_2 \cdot 4H_2O$. $4H_2O$ corresponds to four water molecules and appears as pink crystals with a molecular weight of 197.9 g/mol.

2.1 Preparation of PVA-PEO-$MnCl_2.4H_2O$

To prepare the pure polymeric blend film [PVA-PEO] via the casting method, a specific weight percentage of polyvinyl alcohol (PVA) was combined with a designated weight percentage of polythene oxide (PEO), followed by the addition of 35 ml of distilled water. This mixture was subjected to magnetic stirring for 3 hours at a temperature of 70°C to achieve a homogeneous solution. The solution is subsequently poured into a specialised glass mould positioned on a stable surface and allowed to remain until the solvent evaporates over a duration of 24 hours, resulting in the desired sample film. The composite films (PVA-PEO-$MnCl_2$) were prepared at different weight ratios of 10, 20, 30, 40, and 50 wt%. Table 1 presents the weight percentages utilised in the fabrication of the composite films (PVA–PEO $MnCl_2.4H_2O$). The exact weight ratios of PVA-PEO and $MnCl_2$ salt were determined to manufacture the PVA-PEO-$MnCl_2$ composite films, Table 2 Diagram of typical dimensions of the molds.

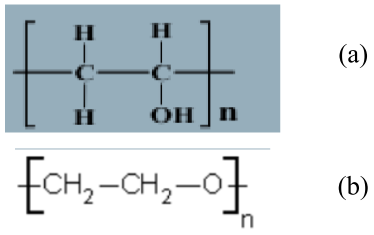

Figure 1: The structural formula of the polymer: a) PVA [6], b) PEO [7].

2.2 Thermal Conductivity

Thermal conductivity of the composite is calculated using Fourier's law. According to Fourier's law, thermal conductivity is given by the equation [8]:

$$Q = - k\, dt/dx. \qquad (1)$$

Where:

- Q: denotes the heat flux, or heat flow, per unit time per unit area;
- k: is the thermal conductivity coefficient;
- dT/dx: is the temperature gradient through the conductive medium.

The units of (Q) and (λ) are (W/m^2) and (W/m.°K), respectively.

The thermal conductivity of a poor heat conducting material in the form of a disk, such as polymer-based materials, can be measured using (Lee's Disc Method).

The thermal conductivity coefficient (k) is determined using the following equation [9]:

$$k\{(T_B-T_A) / d_s\}= e[T_A+ r/2(d_A+ d_s/4)T_A+1/2r(d_sT_B)] \qquad (2)$$

Where e: is the heat flow rate per unit area of the disk (W/m^2.°K).

2.3 Differential Scanning Calorimeter (DSC)

Differential Scanning Calorimeter (DSC) model evo 131 from Sitaram, France). To determine the glass transition temperature T_g and crystalline melting temperature T_m of the polymeric blend and composite films.

Table 1: The weight ratios of composite films (PVA–PEO $MnCl_2.4H_2O$).

Weight Ratio of Additive $MnCl_2.4H_2O$ Salt(wt%)	Weight of (PVA) polymer(g)	Weight of (PEO) polymer(g)	Required Weight of Additive $MnCl_2.4H_2O$ Salt (g)
Pure [PVA-PEO]	0.50	0.50	0
10	0.45	0.45	0.1
20	0.40	0.40	0.2
30	0.35	0.35	0.3
40	0.30	0.30	0.4
50	0.25	0.25	0.5

Table 2: Diagram of typical dimensions of the molds.

Specimen Thickness	Mold standard dimensions	The type of examination or test
80μm	80 mm,20mm	Thermal Conductivity Test
1450μm	80mm,20mm	True Density, Apparent Porosity and Water Absorbance Tests

2.4 Density, Porosity and Water Absorption

2.4.1 True Density

To evaluate the real density, apparent porosity, and water absorption used a Sartorius device of German origin was employed. Apparent density is determined by comparing the test piece with a liquid having a known density (water or mercury). This can be done by weighing the material Archimedes' method (ASTM) test methods:

$$\rho t = \frac{w_1}{w_3 - w_2} * D. \quad (3)$$

Where:

- ρt = real density measured in units (g/cm^3).
- D = density of pure water measured in units (g/cm^3).
- w_1: quantity of dried sample weight in units (g).
- w_2: the sample's weight after being submerged in water in units (g).
- w_3: water-saturated sample weight in units (g).

2.4.2 Apparent Porosity

Then, Apparent porosity may be calculated as the ratio of the open pore volume to total volume [10]:

$$(A.P)\ \% = \frac{w3 - w_1}{w_3 - w_2} * 100\%. \quad (4)$$

(A.P) % = Where:

- A.P: apparent porosity (%).
- w1: quantity of dried sample weight in units (g).
- w2: the sample's weight after being submerged in water in units (g).
- w3: water-saturated sample weight in units (g).

2.4.3 The Water Absorption

After that, the water absorption may be determined by using either "the vacuum/boiling "or "boiling" technique only. However, for vitreous bodies, of less than (1%) water absorption, the difference in the vacuum/boiling and the boiling only technique is critical. it is always possible to apply the following equation to find the water absorption [11]:

$$(W.A)\ \% = \frac{w_3 - w1}{w_1} * 100\%. \quad (5)$$

Where:

- W.A: water absorbency (%).
- w1: quantity of dried sample weight in units (g).
- w2: the sample's weight after being submerged in water in units (g).
- w3: water-saturated sample weight in units (g).

3 RESULTS AND DISCUSSION

3.1 Thermal Characteristics

Figure 2 illustrates the thermal conductivity coefficient of the pure polymeric blend film [PVA-PEO] and polymeric composite films containing MnCl2 salt at various weight ratios, calculated using (1) and (2). The purified polymeric blend film [PVA-PEO] exhibits a thermal conductivity coefficient of 0.000356 W/m·ºK. The incorporation of $MnCl_2 \cdot 4H_2O$ salt at different weight ratios significantly influences the thermal conductivity coefficient. With 10 wt% $MnCl_2 \cdot 4H_2O$ salt, the thermal conductivity coefficient increases to 0.000474 W/m·ºK. Following this, it decreases markedly as the amount of supplementary salt rises.

The differences in the thermal conductivity coefficient arise from the disparities between the matrix material (polymeric blend [PVA-PEO]) and the reinforcing agent, salt. This issue stems from the extensive surface area of the salt [12]. Table 3 displays the thermal conductivity coefficients for all polymeric composite films. The glass transition temperature (T_g) of pure PVA-PEO films and polymer blend films with varying weight ratios of $MnCl_2{\cdot}4H_2O$ was evaluated, as illustrated in Fig. 3 and Table 4. The significant variation in the glass transition temperature arises from the formation of nano-crystalline regions with different diameters and thicknesses within the crystalline domains. This occurs due to the interaction between the salt crystals and the matrix material (PVA-PEO). The glass transition temperature decreases as the mobility of the chains in the salt-reinforced polymeric mixture reduces and salt atoms aggregate in greater quantities [13].

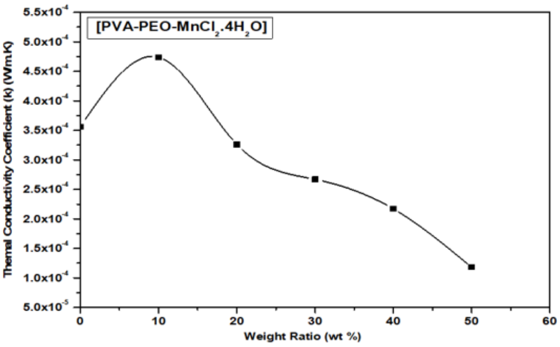

Figure 2: Thermal conductivity coefficient of the composite films [PVA-PEO-$MnCl_2.4H_2O$] as a function to the weight ratio of $MnCl_2.4H_2O$ salt.

The crystalline melting point characteries the properties and stability of a substance [14]. Figure 3 depicts the crystalline melting temperature values for all polymeric composite films, as outlined in Table 5. The crystalline melting point of the purified polymeric blend film [PVA-PEO] is 167.94 °C. When reinforced with $MnCl_2{\cdot}4H_2O$ salt at different weight ratios, the crystalline melting temperature demonstrates abrupt fluctuations relative to the pure polymeric composite film [PVA-PEO]. The variations in the crystalline melting temperature of the pure polymeric composite film [PVA-PEO] suggest that increased crystallinity and structural uniformity diminish as the degree of crosslinking increases [15]. Furthermore, it can be observed that endothermic peaks emerge, indicating the decomposition temperature (Td), which occurs subsequent to the crystalline melting point.

Table 3: Value of the thermal conductivity coefficient of the composite films [PVA-PEO-$MnCl_2.4H_2O$].

[PVA-PEO-$MnCl_2.4H_2O$] k (W/m.ºK)	Weight Ratio of Additive $MnCl_2.4H_2O$ Salt (wt %)
0.000356	Pure [PVA-PEO]
0.000474	**10**
0.000326	**20**
0.000267	**30**
0.000217	**40**
0.000118	**50**

Table 4: Value Tg of [PVA-PEO-MnCl2.4H2O] with weight ratio of MnCl2.4H2O salt.

Weight Ratio of Additive $MnCl_2{\cdot}4H_2O$ Salt (wt%)	[PVA–PEO–$MnCl_2{\cdot}4H_2O$] Tg (°C)
[PVA–PEO]	66.44
10	65.76
20	60.12
30	62.96
40	57.53
50	54.70

Table 5: Value of the crystalline melting temperature of the composite films [PVA-PEO-$MnCl_2.4H_2O$].

Weight Ratio of Additive $MnCl_2{\cdot}4H_2O$ Salt (wt%)	[PVA–PEO–$MnCl_2{\cdot}4H_2O$] T_m (°C)
[PVA–PEO]	167.94
10	243.67
20	147.84
30	100.46
40	170.11
50	100.85

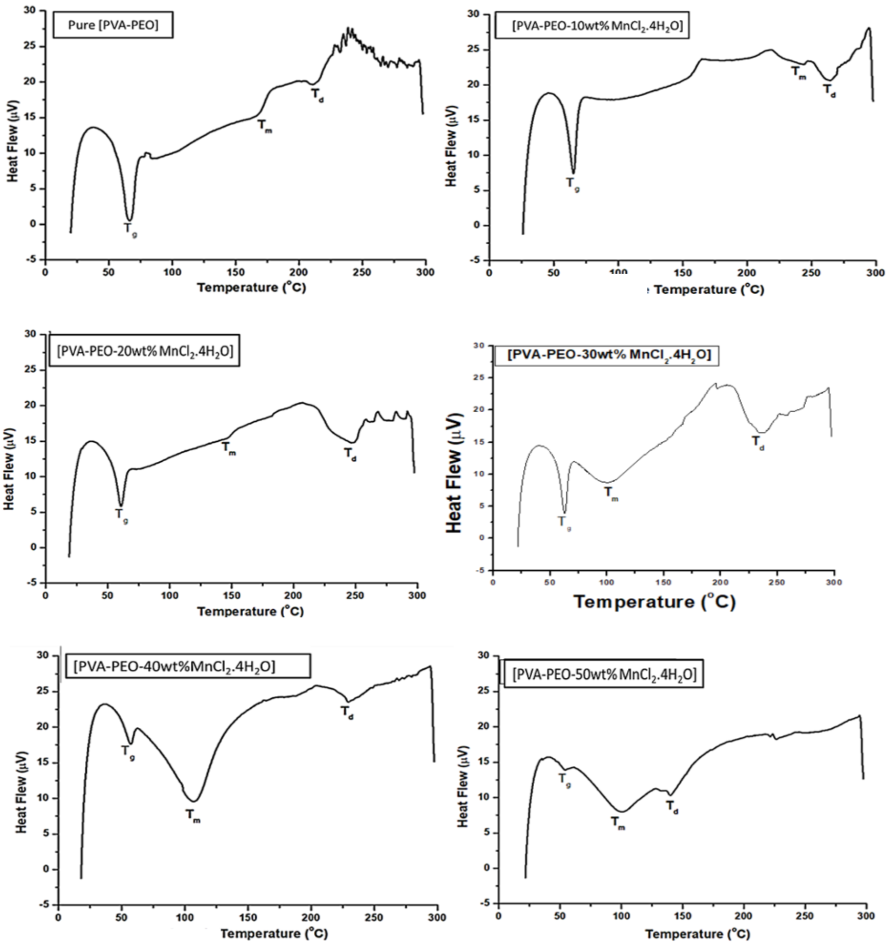

Figure 3: DSC diagram of [PVA-PEO and $MnCl_2.4H_2O$].

3.2 True Density

Figure 4 shows how (3) was used to figure out the true density of the pure polymeric blend film [PVA-PEO] and the polymeric blend films strengthened by MnCl2.4H2O salt at different weight ratios. The figure shows that the pure polymeric blend film [PVA PEO] has a true density of (0.111 g/cm3). When MnCl2.4H2O salt is added in different weight ratios, the real density value increases with the rising weight ratio of the added MnCl2·4H2O salt. Owing to the chemical makeup of salt, which influences the density at a specific temperature, leading to an elevation in density.

The way of immersed the sample in water is significant as it facilitates the proximity of the granular components inside the sample. This elevates the quantity of stacked particles per unit volume of the sample, resulting in increased density when submerged in water; nevertheless, it does not imply that the materials have attained their maximum density. The density increases with rising temperature due to a reduction in voids inside the sample [16]. The actual densities of all the polymeric blend films are presented in Table 6.

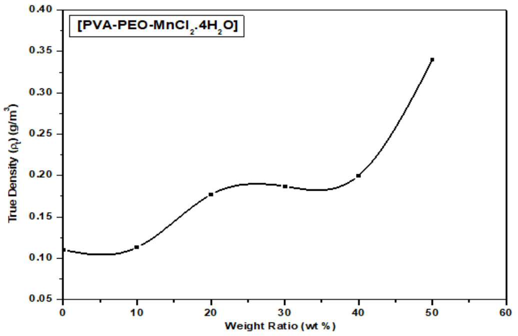

Figure 4: True density of the composite films [PVA-PEO-$MnCl_2.4H_2O$] as a function of the weight ratio of $MnCl_2.4H_2O$ salt.

Table 6: Value True density of the composite film [PVA-PEO-$MnCl_2.4H_2O$].

Weight Ratio of Additive $MnCl_2 \cdot 4H_2O$ Salt (wt%)	[PVA–PEO–$MnCl_2 \cdot 4H_2O$] True Density ρ_t (g/cm³)
[PVA–PEO]	0.111
10	0.113
20	0.177
30	0.187
40	0.200
50	0.340

Figure 5 shows how (4) was used to figure out the different weight ratios of the polymeric blend films strengthened by MnCl2.4H2O salt. The picture shows that the pure polymeric blend film [PVA PEO] has an apparent porosity value of (0.957%). When $MnCl_2.4H_2O$ salt is added in different weight ratios, we can see that the apparent porosity value goes down as the weight ratio of added $MnCl_2.4H_2O$ salt goes up. Because the particles are coming together and breaking up into smaller pieces, and the pores are closing up, the films seem to have less open spaces. There are three main things that affect how porous something seems: temperature, the formation of porosity (open pores), and holes in the films caused by gas release. These factors have the opposite effect on each other [17]. When you put samples in water, the pressure changes, which in turn changes the porosity. The porosity is affected by the raw materials that were used to make them, which are affected by the size and spread of the particles [18]. There are numbers in Table 7 that show how porous all of the polymeric blend films seem to be.

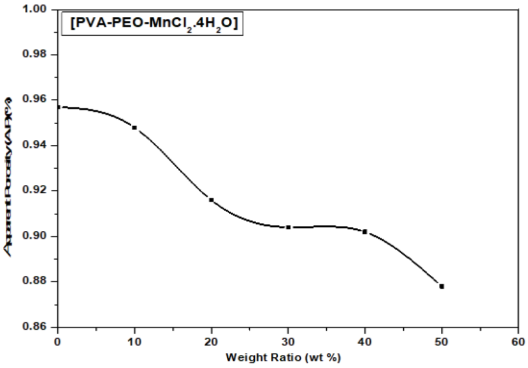

Figure 5: Apparent porosity of the composite films [PVA–PEO–$MnCl_2 \cdot 4H_2O$] as a function of the weight ratio of $MnCl_2 \cdot 4H_2O$ salt.

3.3 Water Absorbance

Figure 6 presents the outcomes of assessing the water absorbance of different polymeric blend films augmented with $MnCl_2 \cdot 4H_2O$ salt, alongside pure polymeric blend films [PVA-PEO] with diverse weight ratios. The figure shows a water absorption rate of 8.554% for the pure [PVA-PEO]. This value decreases with increasing weight percentage of added salt. This happens because the solid phase reacts with the film components, which makes the liquid phase stronger. Phase is very important for understanding the link between how much water a material absorbs and how porous it seems [18], [19]. In Table 8, you can see how much water each polymeric mix screen can hold.

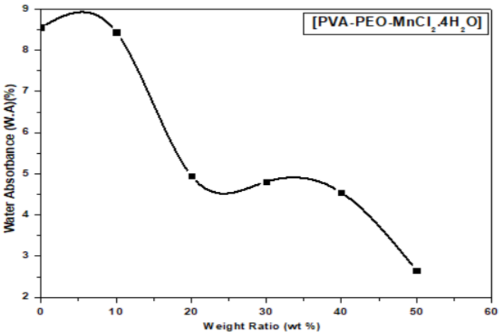

Figure 6: Water absorbance of [PVA-PEO-$MnCl_2.4H_2O$] as a function of the weight ratio of $MnCl_2.4H_2O$ salt.

Table 8: Water absorbance value of the composite films [PVA-PEO-$MnCl_2.4H_2O$].

Weight Ratio of Additive $MnCl_2 \cdot 4H_2O$ Salt (wt%)	[PVA–PEO–$MnCl_2 \cdot 4H_2O$] Apparent Porosity (A.P) (%)
[PVA–PEO]	0.957
10	0.948
20	0.916
30	0.904
40	0.902
50	0.878

4 CONCLUSIONS

In conclusion, the incorporation of $MnCl_2 \cdot 4H_2O$ into the [PVA-PEO] polymer blend produced notable modifications in both thermal and physical properties. The thermal conductivity exhibited an initial enhancement followed by a decline at higher salt loadings, while Tg and Tm values showed irregular shifts, indicating altered chain mobility and crystallinity within the matrix. The progressive increase in true density, accompanied by reduced porosity and water absorbance, reflects a more compact and structurally integrated network. These findings confirm that $MnCl_2 \cdot 4H_2O$ functions as an effective structural and thermal modifier rather than a passive filler, enhancing polymer–salt compatibility and influencing microstructural organization. Overall, the improved stability and tunable properties of the composite films underscore their potential for applications in flexible electronics, solid polymer materials.tests and analyses on pure [PVA-PEO] polymer blend films with different concentrations of $MnCl_2 \cdot 4H_2O$, it was found that the thermal conductivity of the [PVA-PEO-$MnCl_2 \cdot 4H_2O$] composites initially increased and then decreased at higher salt concentrations. The glass transition temperature (Tg) and crystalline melting point (Tm) exhibited irregular reductions compared to the pure blend. Additionally, the density of the composite films increased with the addition of $MnCl_2 \cdot 4H_2O$, while their porosity and water absorption decreased, indicating enhanced structural compactness. These results suggest that $MnCl_2 \cdot 4H_2O$ plays a crucial role in modifying the thermal and physical properties of the [PVA-PEO] polymer matrix, making these composites promising candidates for applications in solid polymer electrolytes, flexible electronic devices, and energy storage systems.

ACKNOWLEDGMENTS

The authors would like to thank the Department of Physics, College of Science, University of Diyala, for their ongoing support and supply of resources for this research.

REFERENCES

[1] R. Mahmood, S. Salman, and N. Bakr, “Optical, thermal properties of cadmium chloride reinforced PVA:PVP blend films,” J. Polymer & Composites, vol. 8, no. 1, pp. 46-52, 2020.

[2] J. Dai, “Advances in developing thermally conductive polymers,” Polymers & Polymer Composites, 2024.

[3] M. A. Shahid and L. H. Sperling, Introduction to Physical Polymer Science. New York: John Wiley, 2006, doi: 10.1080/21663831.2024.2323026.

[4] A. A. Sallal, H. M. Hassan, and M. Ibrahim, “Improving optical properties of polyvinyl alcohol (PVA) and carboxymethyl cellulose (CMC) as polymer blend films (CMC-PVA),” in Proc. 6th Int. Conf. Future Networks & Distributed Systems, Dec. 2022, pp. 652-656.

[5] Al-Ahmad et al., “Thermal characteristics of PVA/PEO blend films,” Hrcak, 2021.

[6] S. Kamath, M. K. Harish Kumar, H. G. Chandramanil, and M. C. Radhakrishna, “PVP influence on PVA crystallinity and optical band gap,” Scholar Research Library, vol. 6, no. 2, pp. 18-21, 2015.

[7] H. Tadokoro, “Structure and properties of crystalline polymers,” Polymer, vol. 25, pp. 147-164, 1984, doi: 10.1016/0032-3861(84)90321-5.

[8] A. Landrok and A. Zakhidov, Heat and Thermodynamics, 4th ed. Addison-Wesley Publishing Company, 1972, pp. 587-592.

[9] Z. Han and A. Fina, “Thermal conductivity of carbon nanotubes and their polymer nanocomposites: A review,” Progress in Polymer Science, vol. 36, pp. 914-944, 2011, doi: 10.1016/j.progpolymsci.2010.11.004.

[10] P. W. Hwrman, Materials Science and Metallurgy, 3rd ed. Reston Publishing Co., Virginia, 1981, pp. 96-100.

[11] S. Rahe, “Study of effect of X-ray on the physical properties of polyvinylpyrrolidone (PVP),” M.Sc. Thesis, University of Mustansiriyah, College of Science, 2004.

[12] I. S. Elashamwi, E. M. Abdelrazek, and A. Y. Yassin, “Influence of $NiCl_2$/$CdCl_2$ as mixed filler on structural, thermal, and electrical properties of PVA/PVP blend,” Brit. J. Appl. Sci. & Tech., vol. 4, no. 30, pp. 4263-4279, 2014.

[13] H. M. Zidan, N. A. El-Ghamaz, A. M. Abdelghany, and A. Lotfy, “Structure and electrical properties of PVA/PVP blend doped with methylene blue dye,” Electrochemical Science, vol. 11, pp. 9041-9056, 2016.

[14] V. Kovacevic, M. Leskovac, and S. Blagojevic, “Morphology and failure in nanocomposites. Part II: Surface investigation,” J. Adhesion Sci. and Tech., vol. 16, no. 7, pp. 1915-1921, 2002, doi: 10.1163/156856102321151478.

[15] B. H. Rabee and A. Hashim, “Synthesis and characterization of carbon nanotubes–polystyrene composites,” Eur. J. Social Sci., vol. 60, no. 2, pp. 229-236, 2011.

[16] R. H. Akbarnejad, V. Daadmehr, F. Sh. Tehrani, F. Aghakhani, and S. Gholipour, “Catalytic effect of the spinel ferrite nanocrystals on the growth of carbon nanotubes,” Magnet and Superconducting Research Lab, Alzahra University, Tehran, no. 12, pp. 1-12, 2011.

[17] S. K. Behera, P. Barpanda, S. K. Pratihar, and S. Bhattacharyya, “Synthesis of magnesium–aluminium spinel from autoignition of citrate–nitrate gel,” Materials Letters, vol. 58, no. 5, pp. 1451-1455, 2004, doi: 10.1016/j.matlet.2003.10.004.

[18] A. M. Bhavikatti, S. Kulkarni, and A. Lagashetty, “Electromagnetic studies of nickel ferrite synthesized by microwave route,” Int. J. Eng. and Tech., vol. 3, no. 1, pp. 687-695, 2011.

[19] F. A. Chiad and A. H. Ali, “Study of the physical properties of a composite material from the aluminum–boron carbide system,” Eng. and Tech. Mag., vol. 28, no. 10, pp. 1-10, 2010.